Epidermal Keratinocyte Depletion during Five Weeks of Radiotherapy is Associated with DNA Double-Strand Break Foci, Cell Growth Arrest and Apoptosis: Evidence of Increasing Radioresponsiveness and Lack of Repopulation; the Number of Melanocytes Remains Unchanged

Authors: Turesson, Ingela, Simonsson, Martin, Hermansson, Ingegerd, Book, Majlis, Sigurdadottir, Sunna, et al.

Epidermal Keratinocyte Depletion during Five Weeks of Radiotherapy is Associated with DNA Double-Strand Break Foci, Cell Growth Arrest and Apoptosis: Evidence of Increasing Radioresponsiveness and Lack of Repopulation; the Number of Melanocytes Remains Unchanged

Ingela Turesson,[a,1,2] Martin Simonsson,[a,2] Ingegerd Hermansson,[b] Majlis Book,[a] Sunna Sigurdadottir,[a] Ulf Thunberg,[a] Fredrik Qvarnström,[a] Karl-Axel Johansson,[c] Per Fessé[d] and Jan Nyman[b]

[a] Department of Immunology, Genetics and Pathology, Experimental and Clinical Oncology, Uppsala University, Uppsala, Sweden; Departments of [b] Oncology and [c] Radiophysics, University of Göteborg, Sahlgrenska University Hospital, Gothenburg, Sweden; and [d] Centre for Research and Development, Uppsala University/Region Gävleborg, Gävle, Sweden

Turesson, I., Simonsson, M., Hermansson, I., Book, M., Sigurdadottir, S., Thunberg, U., Qvarnström, F., Johansson, K-A., Fessé, P. and Nyman, J. Epidermal Keratinocyte Depletion during Five Weeks of Radiotherapy is Associated with DNA Double-Strand Break Foci, Cell Growth Arrest and Apoptosis: Evidence of Increasing Radioresponsiveness and Lack of Repopulation; the Number of Melanocytes Remains Unchanged. *Radiat. Res.* **193**, 481–496 (2020).

During fractionated radiotherapy, epithelial cell populations are thought to decrease initially, followed by accelerated repopulation to compensate cell loss. However, previous findings in skin with daily 1.1 Gy dose fractions indicate continued and increasing cell depletion. Here we investigated epidermal keratinocyte response with daily 2 Gy fractions as well as accelerated and hypofractionation. Epidermal interfollicular melanocytes were also assessed. Skin-punch biopsies were collected from breast cancer patients before, during and after mastectomy radiotherapy to the thoracic wall with daily 2 Gy fractions for 5 weeks. In addition, 2.4 Gy radiotherapy four times per week and 4 Gy fractions twice per week for 5 weeks, and two times 2 Gy daily for 2.5 weeks, were used. Basal keratinocyte density of the interfollicular epidermis was determined and immunostainings of keratinocytes for DNA double-strand break (DSB) foci, growth arrest, apoptosis and mitosis were quantified. In addition, interfollicular melanocytes were counted. Initially minimal keratinocyte loss was observed followed by pronounced depletion during the second half of treatment and full recovery at 2 weeks post treatment. DSB foci per cell peaked towards the end of treatment. p21-stained cell counts increased during radiotherapy, especially the second half. Apoptotic frequency was low throughout radiotherapy but increased at treatment end. Mitotic cell count was significantly suppressed throughout radiotherapy and did not recover during weekend treatment gaps, but increased more than threefold compared to unexposed skin 2 weeks post-radiotherapy. The number of melanocytes remained constant over the study period. Germinal keratinocyte loss rate increased gradually during daily 2 Gy fractions for 5 weeks, and similarly for hypofractionation. DSB foci number after 2 Gy irradiation revealed an initial radioresistance followed by increasing radiosensitivity. Growth arrest mediated by p21 strongly suggests that cells within or recruited into the cell cycle during treatment are at high risk of loss and do not contribute significantly to repopulation. It is possible that quiescent (G_0) cells at treatment completion accounted for the accelerated post-treatment repopulation. Recent knowledge of epidermal tissue regeneration and cell cycle progression during genotoxic and mitogen stress allows for a credible explanation of the current finding. Melanocytes were radioresistant regarding cell depletion. © 2020 by Radiation Research Society

INTRODUCTION

Repopulation of surviving keratinocytes after heavy irradiation of skin areas in mice was first elucidated and quantified in a colony assay developed by Withers (*1*). Before that, Fowler *et al.* had demonstrated in dose-time-fractionation studies on pig skin a reduction of acute skin reactions with prolongation of the overall treatment time, suggesting sparing by repopulation with increasing interval between dose fractions (*2*). The concept of changes in the rate of repopulation during fractionated treatment was initially proposed by Denekamp based on a study of mouse skin, designed with top-up doses (*3*). Importantly, in the interpretation of the outcome from various experimental designs, a distinction should be drawn between repopulation after the end of fractionated doses and repopulation that occurs during the treatment course.

Experimental observations suggest that the rate of keratinocyte depletion is linear and independent of the

fractionation regimen of radiotherapy. However, a few weeks into treatment the depletion rate might decrease, depending on dose per fraction. This was found to be associated with increase in labeling index and interpreted as onset of accelerated repopulation during the treatment course, as Morris and Hopewell demonstrated in a study on pig skin, using daily dose fractions for 6 weeks (4). Archambeau *et al.* confirmed this finding for pig skin irradiated with daily doses of 2 Gy for 6 weeks, from an assessment of mitotic index (5). However, the two studies had an important difference: in contrast to the linear depletion of basal cells from start of treatment, as Morris and Hopewell found (4), Archambeau *et al.* (5) found that the basal cell density remained at control levels for the first 2 weeks of treatment. This distinction is of special interest to the current study, which focuses on the rate of cell loss of basal keratinocytes in human skin during fractionated radiotherapy.

Extensive animal studies in skin, oral mucosa and intestine were then undertaken during the 1980s and 1990s to establish the effect of dose intensity and modulation of cell proliferation on the efficacy of repopulation. These studies have been reviewed in detail by Thames and Hendry (6) and Dörr (7). In the clinical setting of curative radiotherapy for prostate cancer, dose-response relationships were recently established for loss of basal keratinocytes in the epidermis with fraction sizes in the dose range of 0.05–1.10 Gy given daily five times per week over 7 weeks. Keratinocyte loss during treatment with fraction sizes up to 0.44 Gy was clearly exponential, suggesting a constant effect per fraction throughout the treatment period. However, with 1.10 Gy per fraction, the response deviated from an exponential fit 3 weeks into radiotherapy. Surprisingly, an accelerated rate of keratinocyte loss per unit dose was observed over the final 4 weeks of the 7-week treatment period (8).

The immunostaining results in the previous study also revealed that the depletion rate of basal keratinocytes was paralleled by changes in the expression pattern of the p21 protein. The effectiveness of p21 in inhibiting cell cycle progression and proliferation was reflected by the dose-dependent suppression of mitosis throughout the entire treatment period. Indeed, there was no evidence of accelerated repopulation in the basal germinal cell layer of the epidermis at any dose fraction up to 1.10 Gy over the 7-week radiation treatment course. Apoptosis was infrequent during the first treatment week independent of fraction size, but became far more common at 1.10 Gy per fraction during the final treatment week; this finding is associated with a pronounced increase in the number of DNA double-strand break (DSB) foci per basal keratinocyte. Furthermore, DSB foci persisted at 24 h after dose delivery and accumulated with repeated daily dose fractions in the range 0.05 to 1.10 Gy (9).

Based on these results, we hypothesized that cell cycle arrests that do not recover between daily dose fractions

allow DNA damage to accumulate in cells at each specific checkpoint, i.e., before the G_1/S and G_2/M transitions. The p21 protein functions as a major regulator of both of these transitions (10–12). The accumulation of unrepaired DNA damage might increase the risk of permanent cell cycle arrest or apoptosis at each cell cycle checkpoint. In this scenario, premitotic elimination of cycling cells might become successively more important during the radiotherapy course. There is a possibility that, subsequent to a permanent arrest, cells exit the cell cycle and migrate upwards into the differentiated cell layers (13, 14). This pathway may be viewed as an alternative event to mitotic death that results in depletion of basal keratinocytes. Apoptosis as a consequence of mitotic failure is expected in epithelial cells when a patient is undergoing radiotherapy. Otherwise, apoptosis as a primary mode of death is considered rare in this cell type (15, 16).

In the current study we further investigated the issue of the keratinocyte response during and after radiotherapy by looking at various dose fractionations for breast cancer patients as adjuvant treatment. Keratinocyte loss, DSB foci, growth arrest, mitosis and apoptosis were quantified (8, 9, 17).

Recently, we also established the response of interfollicular melanocytes in epidermis in the dose range 0.05 to 1.10 Gy given daily for 7 weeks (18). Independent of dose, the number of melanocytes remains unchanged over the treatment period. We identified a subset of undifferentiated melanocytes before irradiation, which responded with differentiation in a hyper-radiosensitive manner below 0.3 Gy per fraction. Here, we count the melanocyte number in interfollicular epidermis in the same tissue sections as were assessed for keratinocytes after adjuvant radiotherapy schedules.

MATERIALS AND METHODS

Clinical Assay

Thirty-one breast cancer patients who had undergone mastectomy were recruited for this study. Sixteen patients were recruited between 1988 and 1993 (group 1) and received radiotherapy to the thoracic wall with prescribed daily dose fractions of 2.0 Gy for either 4 weeks (8 patients) or 5 weeks (8 patients); thus, group 1 patients received a total radiation dose of 40 or 50 Gy, respectively. These patients were irradiated with 6 to 14 MeV electrons, with the energy adapted to the thickness of the thoracic wall. A 1-cm tissue-equivalent bolus was given to all patients to obtain a full dose at the skin surface. These patients are a subgroup of those in an earlier published study (19). A second group of 15 post-mastectomy breast cancer patients was recruited between 2005 and 2007 (group 2). Between the two study periods the treatment technique was changed. In group 2, radiotherapy to the thoracic wall was applied using opposed tangential photon beams, 5 MV, plus a 5-mm bolus in a 5- to 10-cm broad strip covering the surgical scar. In this area, the skin received the prescribed dose of 2.0 Gy per fraction (ICRU50), which was given daily for 5 weeks for a total dose of 50 Gy. All recruited patients allowed the collection of skin biopsies before, during and after completion of their treatment course. Punch biopsies 3 mm in diameter were taken under local anesthesia (lidocaine hydrochloride 5 mg/ml without adrenaline).

Biopsies from group 2 patients were taken from skin in the area under the bolus to ascertain a dose fraction of 2.0 Gy to the skin. All biopsies were coded. For group 1 patients, one biopsy was collected from an unexposed area 5 cm outside the thoracic radiation field at 2 weeks of treatment when the first biopsy was taken within the field. For group 2 patients, two control biopsies were sampled within the planned thoracic field prior to the computed tomography (CT) examination that was performed before the start of radiotherapy.

Multiple biopsies were sampled at predetermined intervals during and after completion of treatment over 20 weeks at most. The distance between adjacent biopsies was at least 2 cm. Biopsies taken during the radiotherapy course were sampled at approximately 24 h after the previous fraction (group 1) or 30 min after radiation dose fraction was administered (group 2). All biopsies were fixed immediately after collection in 4% formaldehyde and embedded in paraffin. A total of 240 biopsies were assessed from these 31 patients.

Approval for both study groups was obtained from the Ethics Committee at the University of Gothenburg (Gothenburg, Sweden). Written informed consent was obtained from all patients prior to participation.

Immunohistochemistry

Three tissue sections, each 4 μm thick, were taken from various levels of each biopsy and mounted on a SuperFrost™ Plus slide (Menzel-Gläser, Germany). The slides were dried at 37°C overnight. Immunohistochemical staining of p21, 53BP1 and mitotic marker was performed using a Ventana Benchmark® automated/IHC stainer and the Ventana iView™ DAB Detection Kit (Ventana Medical Systems, Tucson, AZ) plus subsequent manual counterstaining with Meyers HTX. The following primary antibodies were used: anti-p21-Waf-1, EA10 (1:50; Calbiochem, San Diego, CA); for mitosis, the HTA28 antibody, which detects phosphorylated histone H3 at serine 28 (1:200; Abcam, Cambridge, UK); and for 53BP1 foci, anti-53BP1 (1:2,000; Bethyl Laboratories, Montgomery, TX).

Manual immunofluorescence staining of 53BP1 foci and γ-H2AX foci was performed using anti-53BP1 (1:400; Bethyl Laboratories) and a phosphospecific mouse monoclonal antibody specific for γ-H2AX (1:100; Upstate Biotechnology, Charlottesville, VA). Alexa 488 goat anti-rabbit antibody and Alexa 555 goat anti-mouse antibody (1:100; Molecular Probes®, Eugene, OR) were used for secondary detection. Apoptosis was detected by γ-H2AX staining as described elsewhere (8, 17).

All stainings were evaluated using the same light microscope (Nikon Eclipse E400; Tokyo, Japan).

Assessment of the Keratinocyte and Melanocyte Response

The keratinocyte response in the basal germinal cell layer of the epidermis was assessed in biopsies (n = 240) from all 31 patients. Tissue sections were stained with hematoxylin and eosin (H&E) and periodic acid-Schiff. Basal keratinocytes were counted manually at high power (1,000×), and counting was restricted to the interfollicular epidermis. Only cells that were attached to the underlying basement membrane were counted. Basal keratinocytes were identified through their desmosomes (20); these are unequivocally visualized in the high magnification used. Melanocytes were recognized morphologically and excluded from the count and recorded separately by author Fessé. The total number of germinal keratinocytes and melanocytes per mm of basal membrane was determined.

To ensure consistency in determination of the keratinocyte response between groups 1 and 2, a reassessment was performed for the group 1 patients by the same person who assessed the group 2 patients (Hermansson).

The basal cell density was previously also determined for 2 and 4 fractions per week during five weeks, as well as for 50 Gy given in 2.5 weeks (2 × 2.0 Gy/day, 8-h interval) from patients recruited between 1988 and 1993 (19). The same clinical setting was used as described

above for the group 1 patients. To allow comparison of the keratinocyte response of these schedules with daily 2 Gy fractions, a reassessment excluding the melanocytes was done by the same person (author Hermansson). The number of melanocytes was counted separately by Fessé.

Assessment of Keratinocyte Growth Arrest

Biopsies (n = 144) from 15 patients (group 2) were assessed for nuclear expression of the p21 protein by the author Sigurdadottir. All keratinocytes in the basal layer with any detectable p21 staining in the nucleus were counted manually at high power (1,000×). The number of stained cells per mm of interfollicular epidermis was recorded (Fig. 1 A). An independent counting of p21-negative keratinocytes at the end of treatment was performed by Fessé. This was done to ascertain a separation of the p21-negative keratinocytes and the melanocytes which mostly do not stain for p21.

Assessment of Cell Proliferation

Biopsies (n = 197) from 6 patients in group 1 (50 Gy) and from all 15 patients in group 2 (50 Gy) were assessed for cell proliferation by assessing mitotic frequency. Phospho-H3 staining identified all stages of mitosis in tissue sections (21). Because of the scarcity of mitotic events, all stained keratinocytes in the basal and suprabasal layers were counted, which also mitigated any uncertainty about the exact location of the mitotic cell. Manual counting was performed at high power (1,000×), and the number of stained cells per mm of interfollicular epidermis was determined (Fig. 1A).

Assessment of DSB Foci

DSBs were detected using the surrogate markers γ-H2AX (22, 23) and 53BP1 (24, 25). Manual quantification of 53BP1 foci was performed by Hermansson at high power (1,000×) in immunohisto-chemically stained sections. The number of distinct foci per cell was determined for 100 consecutive basal keratinocytes, omitting the melanocytes, in one tissue section and repeating the counting in a second tissue section. Thus, the foci in 200 cells were counted in each biopsy. Biopsies (n = 197) from 6 patients in group 1 and 15 patients in group 2 were assessed; thus, 53BP1 foci were manually counted in 39,400 cells (Fig. 1A).

The entire epidermis was assessed in the image analysis of DSB foci. All images of sections that were immunostained to detect 53BP1 and γ-H2AX were acquired using a Spot Insight Color CCD camera (Diagnostic Instruments, Sterling Heights, MI) connected to a Nikon Eclipse E400 microscope equipped with a 40× objective and G-2A, FITC, and UV-2A filters (Nikon Corporation). The microscope light source was calibrated prior to cell image acquisition. The uniformity of the light field was monitored by lamp position adjustments, and intensity variations were monitored by Alexa 555 fluorescent microspheres mounted on a microscope slide (Molecular Probes). The number of foci per nuclear area was determined by digital image analysis as described elsewhere (26, 17). 53BP1 and γ-H2AX foci were analyzed in biopsies (n = 144) from 15 patients (group 2) (Fig. 1 C), and three sections were analyzed per biopsy. Foci in all nucleated cells in the section, including melanocytes, were assessed.

We also investigated the influence of the fixation time in formaldehyde on the number of foci detected with 53BP1 and γ-H2AX staining. Eleven biopsy pairs were collected; one member of each pair was fixed for one day and the other for four days.

Assessment of Cell Death

Biopsies (n = 144) from 15 patients (group 2) were assessed for apoptotic cell death. Intense immunofluorescent homogeneous nuclear staining with γ-H2AX was used as a marker of apoptosis (8, 17). The dose dependence of apoptotic events was determined by manual
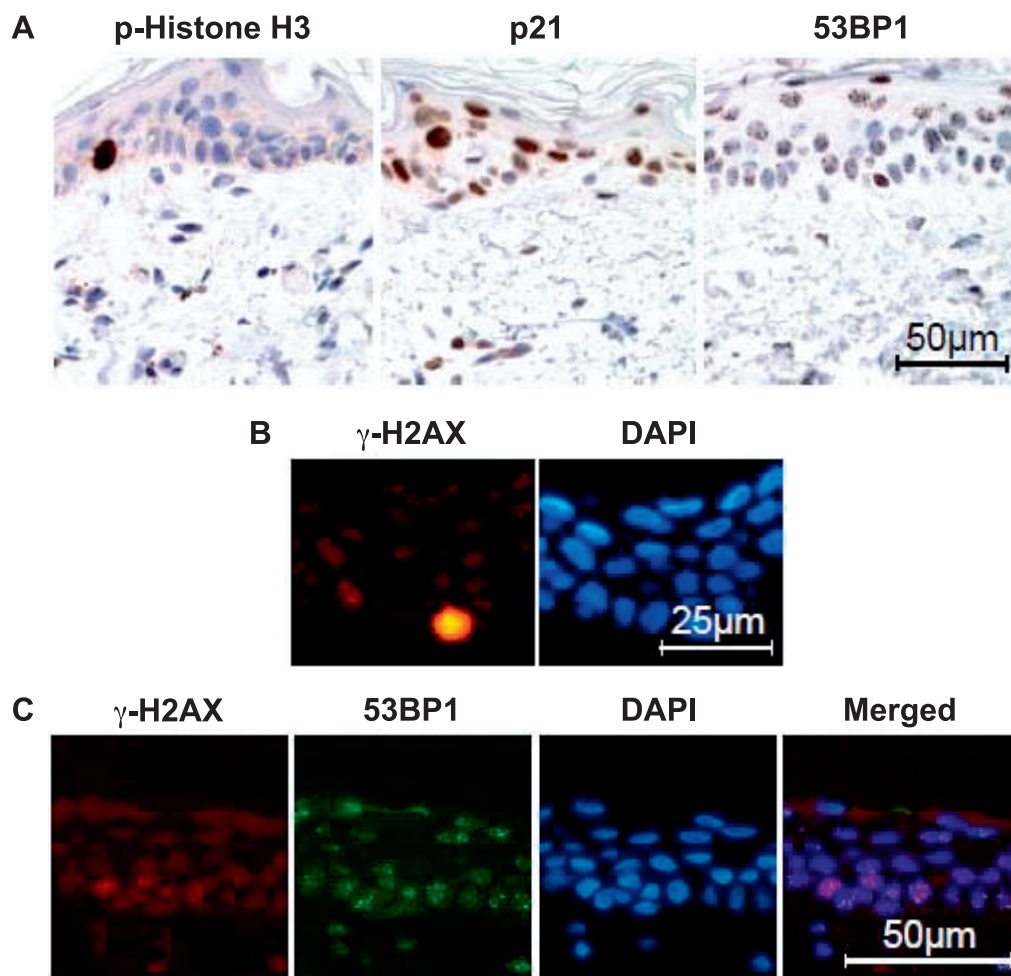
FIG. 1. Representative immunohistochemical staining of biopsy specimen from a breast cancer patient undergoing radiotherapy. Panel A: p-Histone H3, p21 and 53BP1, stained by DAB/HTX, were used as surrogate markers to determine mitotic frequency, cell cycle checkpoint activation, and DNA double-strand break (DSB) density, respectively. Panel B: Apoptotic frequency was assessed by counting a subset of γ-H2AX-positive cells that showed intense homogeneous nuclear staining. Panel C: DNA DSBs were quantified using digital image analysis of immunofluorescence staining of γ-H2AX and 53BP1 within the nuclear regions, as defined by DAPI staining.

counting of basal and suprabasal apoptotic cells in γ-H2AX-stained sections. Because of the scarcity of epidermal apoptosis, at least six tissue sections per biopsy were counted. The length of the basal membranes was measured manually in all sections in corresponding images of DAPI nuclear staining (0.4 μg/ml; Molecular Probes) (Fig. 1B).

RESULTS

Keratinocyte Response

The basal keratinocyte density (BKD) was plotted against time on a log-linear scale (Fig. 2). For group 1 patients, the mean value for control biopsies was 129.4 (SE 2.4) cells per mm. For the group 2 patients, no significant difference in BKD was found in the two unexposed control biopsies compared to biopsies taken 30 min after the first fraction of 2 Gy radiotherapy. Therefore, the mean value from assessing three biopsies per patient was used as the control

BKD, determined as 130.6 (SE 2.4) cells per mm. For all 31 patients, the mean value of 129.9 (SE 1.7) cells per mm was adopted for unexposed skin.

The BKD declined over time during the five weeks of treatment and reached a minimum at one week after the end of radiotherapy. The nadir was followed by a very rapid increase in BKD and complete recovery at two weeks after treatment.

Of note, a flat response was observed over the first 2 weeks of treatment, and only 9.1 basal keratinocytes per mm disappeared; thereafter, a steep response was recorded. Indeed, the decline in BKD during treatment showed a striking deviation from an exponential curve. The number of basal keratinocytes at the final fraction at five weeks was 68.4 (SE 4.4) cells per mm; the value at 6 weeks was significantly lower ($P < 0.008$, sign test). The nadir was 55.4 (SE 5.7) cells per mm.
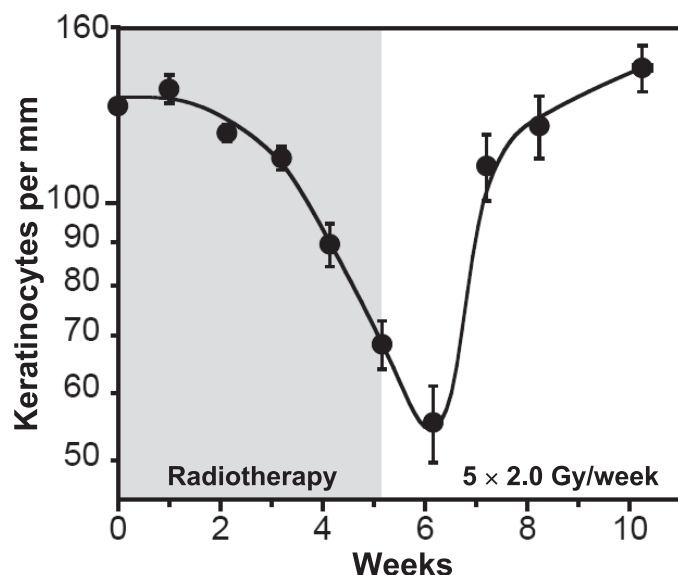
FIG. 2. The keratinocyte response in the basal layer from biopsy samples from breast cancer patients undergoing radiotherapy with 50 Gy in 5 weeks. Vertical error bars indicate the standard error of the mean for basal keratinocyte density (BKD). Horizontal error bars indicate the standard deviation of the biopsy acquisition time, but in this case hidden behind the symbols.

A separate evaluation of the decline rate of basal keratinocytes for the group 1 patients revealed an initial weak response followed by increasing cell loss rate (Fig. 3A). The nadir occurred at 6 weeks and was 52.8 (SE 4.7) cells per mm. The eight patients who received 40 Gy contribute with biopsy data collected only up to 4 weeks from start of radiotherapy.

The depletion rate of basal keratinocytes during the 5-week radiotherapy course given with hypofractionation confirmed a biphasic pattern, with almost no cell loss the first weeks followed by pronounced cell loss during the second part of radiotherapy (Fig. 3C and D). With 2.4 Gy fractions delivered four times per week (Wednesday treatment free) the BKD reached nadir, 65.9 (SE 6.7) cells per mm, 1 week after the end of radiotherapy. With 4.0 Gy fractions given two times per week (fraction interval 3 or 4 days) the BKD reached nadir, 57.4 (SE 5.3) cells per mm, at the end of treatment.

During the 2.5-week radiotherapy course given with 2×2.0 Gy per day to 50 Gy, the keratinocyte cell loss was as low as for daily 2.0 Gy fractions (Fig. 3A and B). Thereafter, the rate of cell depletion increased, but less than for 2.0 Gy per day. The BKD nadir, 73.7 (SE 10.2) cells per mm, occurred at 6 weeks from start of treatment, as was the case for 2.0 Gy per day. Of note, the BKD at nadir was significantly less with 50 Gy in 2.5 weeks compared to 50 Gy in 5 weeks ($P < 0.01$).

For the fractionation schedules shown in Fig. 3, the basal cell density, without distinguishing the melanocytes, published elsewhere (19). In the reassessment the number of melanocytes was determined over the treatment period

and the subsequent weeks for all four radiotherapy schedules. The current determination of BKD was substantially more accurate and specific for keratinocytes by careful recognition and exclusion of melanocytes situated in the inter-follicular basal layer. All assessments of the immuno-histochemical stainings presented were performed at 1,000× magnification to allow for identification of desmosomes, which are unique to keratinocytes.

Melanocyte Response

Quantification of interfollicular melanocytes per mm for the various fractionation schedules is shown in Fig. 4. There was no significant change of the melanocyte numbers during radiotherapy or after treatment for any of the fractionation schedules. The average was 15.0 (SE 0.48) per mm.

Growth Arrest

The expression of p21 protein was assessed for the 15 patients in group 2. The number of p21-positive keratinocytes in unexposed control biopsies was low throughout the basal layer, 1.40 (SE 0.27) cells per mm. During the 5-week treatment, there was an accumulation of p21-positive cells (Fig. 1A), and the intensity of the nuclear staining increased (data not shown). When the number of p21-positive cells was plotted against time using a linear-linear scale, there was a biphasic increase over the treatment period (Fig. 5A). The increase in the fraction of p21-positive cells was more prominent during the second half of the treatment than in the first part of radiotherapy. At 2 weeks, only 17.9 (SE 2.8) p21-positive cells of 120.0 (SE 5.8) basal keratinocytes per mm were observed. At 5 weeks, 53.7 (SE 5.0), p21-positive cells per mm out of 71.8 (SE 6.0) basal keratinocytes per mm were recorded. Of note, in a subpopulation of basal keratinocytes at the end of treatment, p21-staining was scored negative by Sigurdadottir. A reassessment of unequivocally p21-negative keratinocytes at 5 weeks was performed by Fessé. The mean number was 1.5 (SE 0.36) cells per mm. The p21-negative cells were mostly evenly distributed, but occasionally appeared pairwise. A continuous fall in p21-stained cells was observed after completion of radiotherapy. Growth arrest mediated by p21 is expected to direct basal keratinocytes to differentiation and keratinization (13, 14), as shown in Fig. 5B. In contrast to the basal keratinocytes, nearly all interfollicular melanocyte nuclei were p21-negative.

Cell Proliferation

All stages of mitosis were detected reliably using phospho-H3 staining (Fig. 1A). The number of mitotic cells per mm counted during and after the 5-week treatment period is shown in Fig. 6. Few mitotic events were observed in the unexposed skin [0.59 (SE 0.11) cells per mm]. It was clear that mitosis was suppressed during the entire treatment
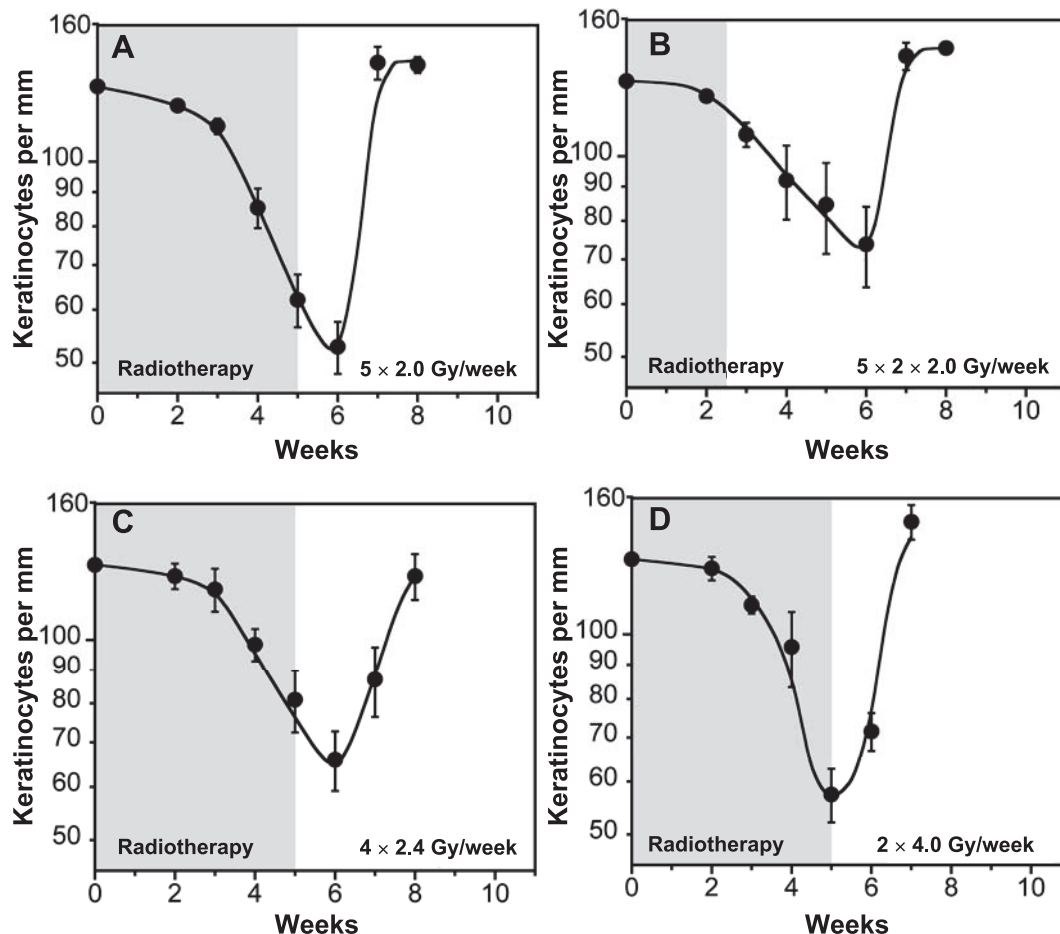
FIG. 3. The keratinocyte response in the basal layer from biopsy samples from breast cancer patients undergoing radiotherapy at: 50 Gy in 5 weeks (16 patients; panel A); 50 Gy in 2.5 weeks (5 patients; panel B); 48 Gy in 5 weeks (5 patients; panel C); and 40 Gy in 5 weeks (5 patients; panel D). Vertical error bars indicate the standard error of the mean for BKD.

period. The lowest value, 0.12 (SE 0.05) cells per mm, was observed at 2 weeks of radiotherapy. Thereafter, a slight but consistent increase was observed until the final fraction at 5 weeks, at which time there were 0.25 (SE 0.08) mitotic cells per mm. This value was still significantly lower than the number of mitotic cells in unexposed skin ($P < 0.007$, sign test; $P = 0.004$, t test).

The effect on the mitotic frequency of the 72-h weekend gap in treatment was estimated by analyzing 15 pairs of biopsies from the group 2 patients, with one of each pair taken on a Friday and the other on the following Monday. There were 0.19 (SE 0.05) and 0.07 (SE 0.03) mitotic cells per mm for biopsies taken on Friday and Monday, respectively. Separate analyses for weekend gaps during weeks 1–2 and weeks 3–4 did not differ. Thus, there was a persistent suppression of mitosis during the weekend gaps throughout the 5-week treatment period.

In contrast, a very rapid increase in the number of mitoses was observed after completion of radiotherapy. The peak value of 2.2 (SE 0.45) mitotic cells per mm was recorded 2 weeks after the end of radiotherapy. Thereafter a rapid decline was observed over the following week. Not until

approximately 10 weeks after completion of treatment did the mitotic frequency reach the value of unexposed skin.

Mitotic cells were well separated among the basal cells, i.e., no mitotic clusters were observed; therefore, no evidence of cell regeneration limited to rapid repopulation within colonies could be detected during or after the radiotherapy course.

DSB Foci

The number of DSB foci per cell, manually counted over the examined period in 53BP1-immunostained basal keratinocytes, is shown in Fig. 7. During the 5-week treatment course, the number of DSB foci per cell at 30 min after delivered dose fractions was determined from the 15 patients in group 2. In the unexposed epidermis, there were 1.4 (SE 0.1) 53BP1 foci per basal keratinocyte. After the very first fraction of 2.0 Gy, the number of 53BP1 foci per cell was 4.8 (SE 0.2). Significantly fewer foci per cell [3.8 (SE 0.3)] were recorded for dose fractions delivered during the first and second weeks of treatment ($P < 0.003$, sign test; $P = 0.008$, t test). The decrease was followed by a
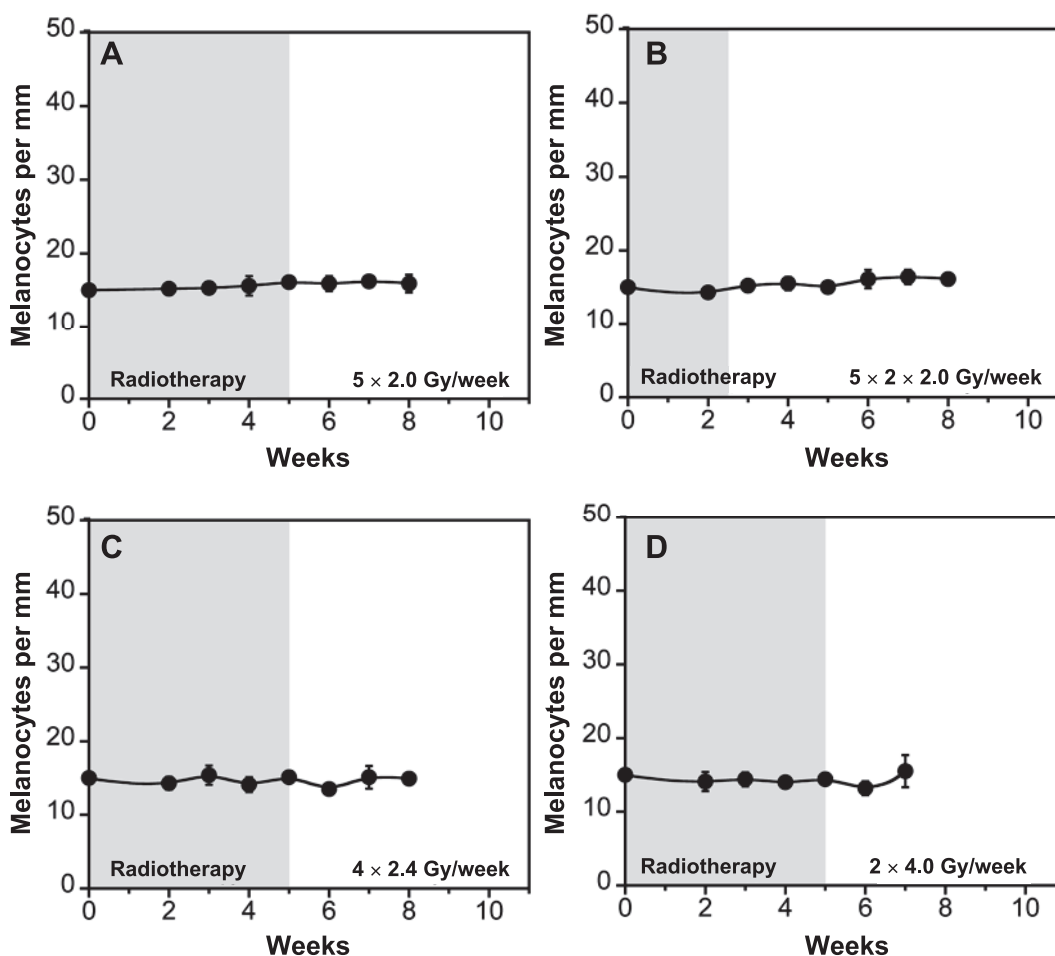
FIG. 4. The melanocyte response in the interfollicular basal layer from biopsy samples from breast cancer patients undergoing radiotherapy at 50 Gy in 5 weeks (5 patients; panel A); 50 Gy in 2.5 weeks (5 patients; panel B); 48 Gy in 5 weeks (5 patients; panel C); and 40 Gy in 5 weeks (5 patients; panel D). Vertical error bars indicate the standard error of the mean for the number of melanocytes per mm.

gradual increase over the remaining 3 weeks. At completion of radiotherapy, 6.6 (SE 0.5) 53BP1 foci per cell were observed, which was significantly higher than that counted after the very first fraction ($P < 0.007$, sign test; $P = 0.004$, t test).

Persistent foci between dose fractions and a trend of accumulation of foci towards the end of treatment were observed at the assessment 24 h after the preceding fraction of 6 patients from group 1 receiving 50 Gy. The mean number of 53BP1 foci per basal keratinocyte was 1.4 (SE 0.2) in the control biopsies. At 2 to 3 weeks and at 4 to 5 weeks, there were 1.8 (SE 0.2) and 2.2 (SE 0.7) 53BP1 foci per cell, respectively.

The decline of foci after the delivery of 50 Gy radiation in 5 weeks was based on assessments of all available biopsies from group 1 and 2 patients. One week after the end of radiotherapy, the number of 53BP1 foci per keratinocyte in the basal layer reached that of unexposed skin (Fig. 7).

From the immunofluorescence staining and digital image analysis, determination of the average number of DSB foci per nuclear area for all nucleated cells in the epidermis was performed for the 15 patients from group 2. Figure 8 shows the number of 53BP1 foci and γ-H2AX foci at 30 min after delivered dose fractions over the 5-week treatment and the foci decline after the end of radiotherapy. In the control biopsies, the foci density was higher for 53BP1 compared to that of γ-H2AX. Beyond that, the number of foci per nuclear area was very similar for 53BP1 and γ-H2AX. A gradual increase in DSB foci from 2 weeks until the end of radiotherapy was evident for 53BP1 ($P = 0.005$, t test), and a similar trend was observed for γ-H2AX ($P = 0.19$, t test). A less rapid decline in foci after the end of radiotherapy was noted for 53BP1 compared to γ-H2AX, which almost reached that of unexposed skin at 1 week. Persistent 53BP1 foci were observed up to 5 weeks after the end of radiotherapy.

Formaldehyde fixation time affects the number of foci detected with γ-H2AX staining, with fewer foci detected with longer fixation times (17). In Fig. 9, the difference between the mean number of foci after 1 day (11 biopsies) and after 4 days (11 biopsies) of fixation is shown for γ-H2AX and 53BP1 double-staining. The longer fixation time
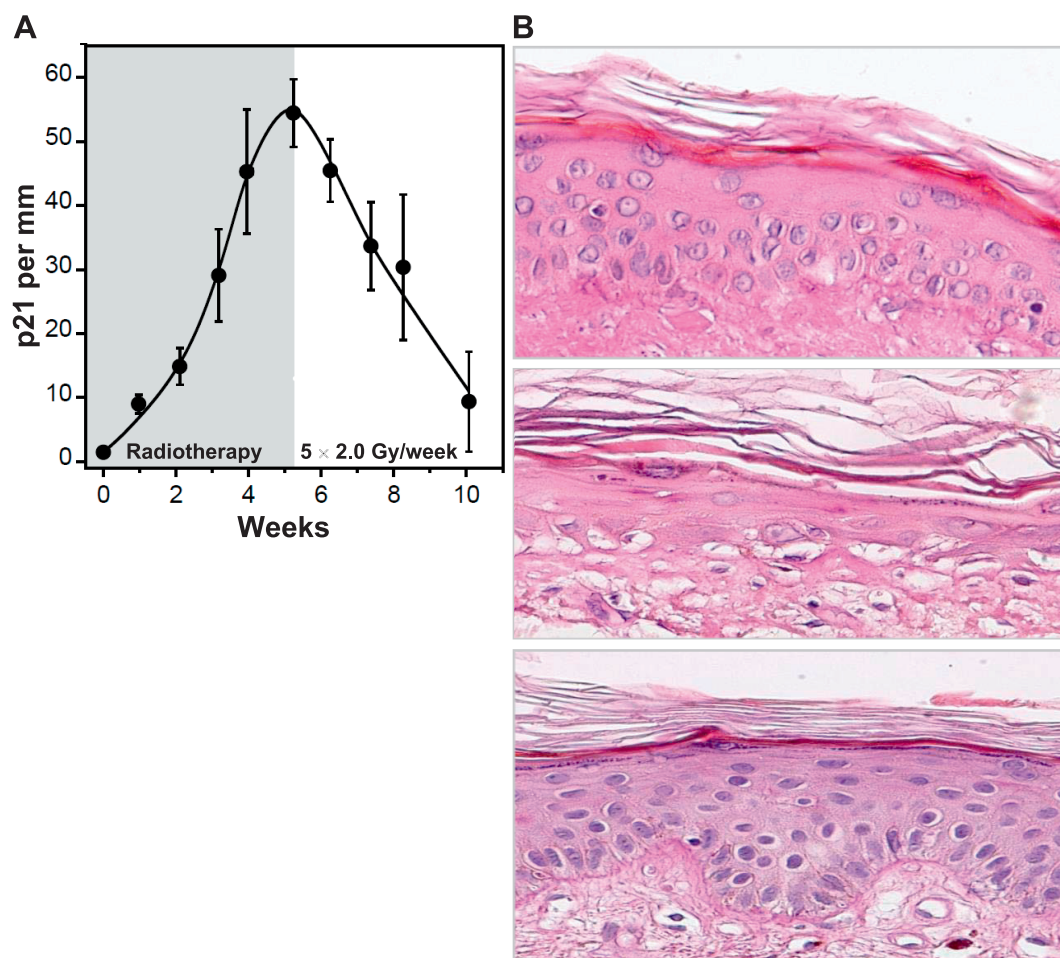
FIG. 5. Panel A: Growth arrest of keratinocytes in biopsy samples from breast cancer patients undergoing radiotherapy. Vertical error bars indicate the standard error of the mean for p21 per mm of the sample. Horizontal error bars indicate the standard deviation of the biopsy acquisition time, but are hidden behind the symbols. Panel B: Skin morphology before treatment (upper panel), at the end of treatment (middle panel), and at 2 weeks after treatment (lower panel).
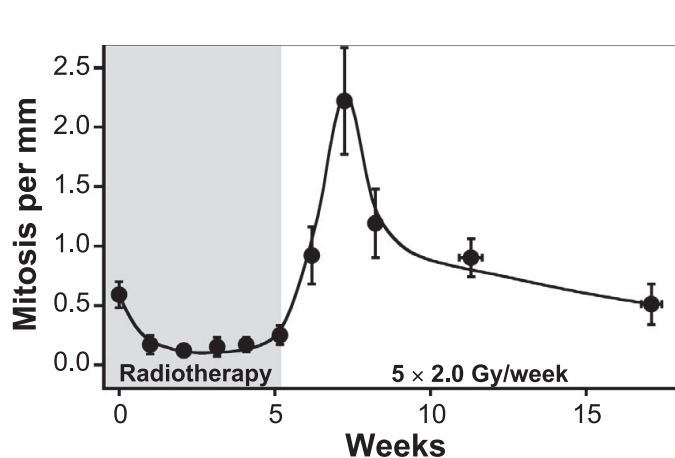

FIG. 6. Cell proliferation in biopsy samples from breast cancer patients undergoing radiotherapy. Vertical error bars indicate the standard error of the mean for phospho-H3-positive cells per mm of the sample. Horizontal error bars indicate the standard deviation of the biopsy acquisition time, but are mostly hidden behind the symbols.
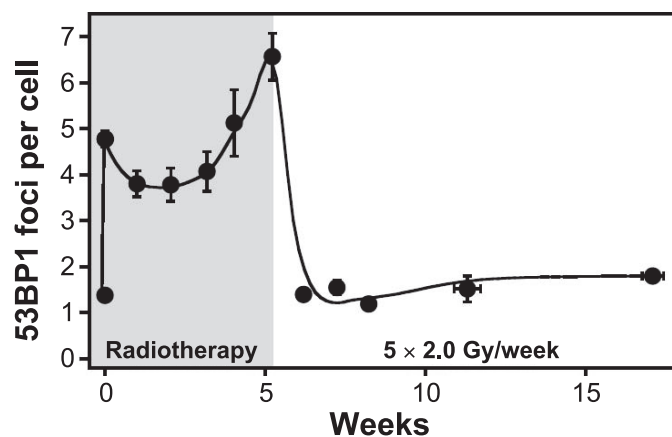

FIG. 7. Manual scoring of 53BP1 foci in biopsy samples from breast cancer patients undergoing radiotherapy 30 min after daily dose fractions of 2 Gy. Vertical error bars indicate the standard error of the mean for 53BP1 foci per cell. Horizontal error bars indicate the standard deviation of the biopsy acquisition time, but are mostly hidden behind the symbols.
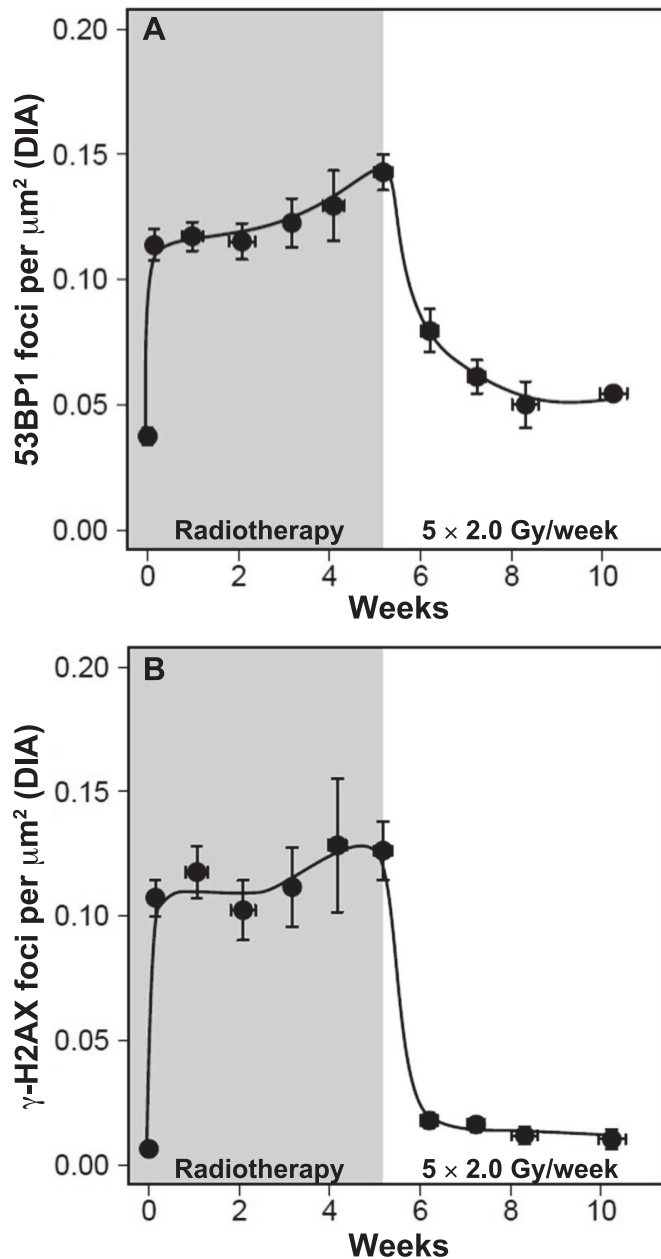
FIG. 8. Panel A: 53BP1 foci determined using digital image analysis in biopsy samples from breast cancer patients undergoing radiotherapy. Vertical error bars indicate the standard error of the mean for 53BP1 foci per nuclear area. Horizontal error bars indicate the standard deviation of the biopsy acquisition time. Panel B: γ-H2AX-positive foci determined by digital image analysis in biopsy samples from breast cancer patients undergoing radiotherapy. Vertical error bars indicate the standard error of the mean for γ-H2AX-positive foci per nuclear area. Horizontal error bars indicate the standard deviation of the biopsy acquisition time.

significantly reduced the number of γ-H2AX foci but not the number of 53BP1 foci. In particular, a reduction in γ-H2AX-positive foci is expected for biopsies collected just before weekend breaks, which, for logistical reasons, were fixed 3 or 4 days. Thus, the formaldehyde fixation time is a confounding factor that reduces the sensitivity to quantification of DSB with the γ-H2AX method.
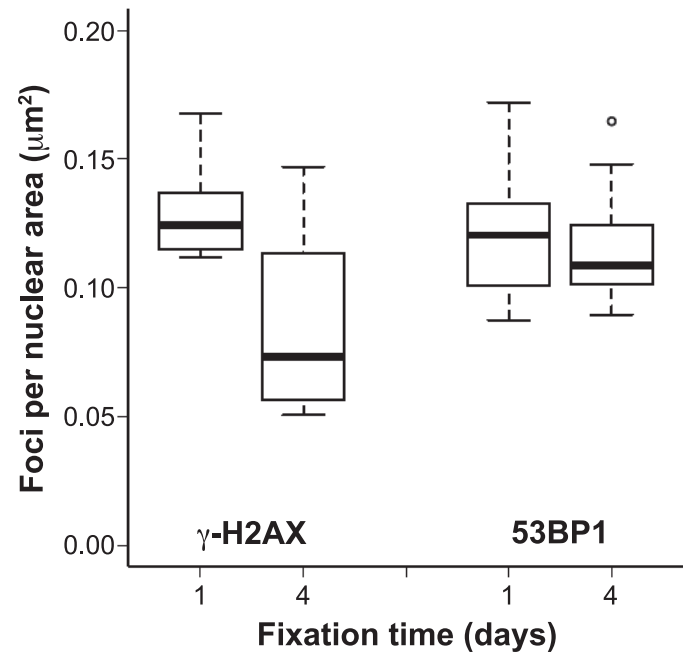

FIG. 9. Effect of formaldehyde fixation time on the number of foci detected by immunofluorescence staining and digital image analyses of γ-H2AX (left side) and 53BP1 (right side) in biopsy samples from breast cancer patients undergoing radiotherapy. Longer fixation time reduced the number of foci detected with γ-H2AX staining, but the number of 53BP1 foci was unaffected.

Apoptosis

Apoptotic cells were identified among the basal and suprabasal keratinocytes by bright and homogeneous staining with γ-H2AX, (8, 17) (Fig. 1 B). Apoptotic count for the 15 patients in group 2 during and after radiotherapy is shown in Fig. 10. The number of apoptotic events prior to treatment was low, at 0.13 (SE 0.15) cells per mm. Apoptosis increased threefold during the first 2 weeks of treatment. Towards the end of radiotherapy, there was a substantial ~10-fold increase in apoptotic cells compared to pretreatment. After completion of radiotherapy, this level persisted for a couple of weeks and then declined in the subsequent weeks, but did not entirely reach pretreatment numbers (Fig. 10).

DISCUSSION

Dose-response in Keratinocyte Depletion

The current study showed how germinal keratinocytes in the interfollicular epidermis respond to daily exposure of 2.0 Gy over 5 weeks, and also after hypo- and accelerated fractionation, as well as their behavior during the recovery phase after the radiotherapy course. The decline in basal keratinocytes over the treatment period was not exponential, as would be expected if each dose fraction in the radiotherapy course had an equal effect. Rather, the pattern of keratinocyte loss on a log-linear scale was approximately biphasic, illustrating an initial low depletion rate of basal
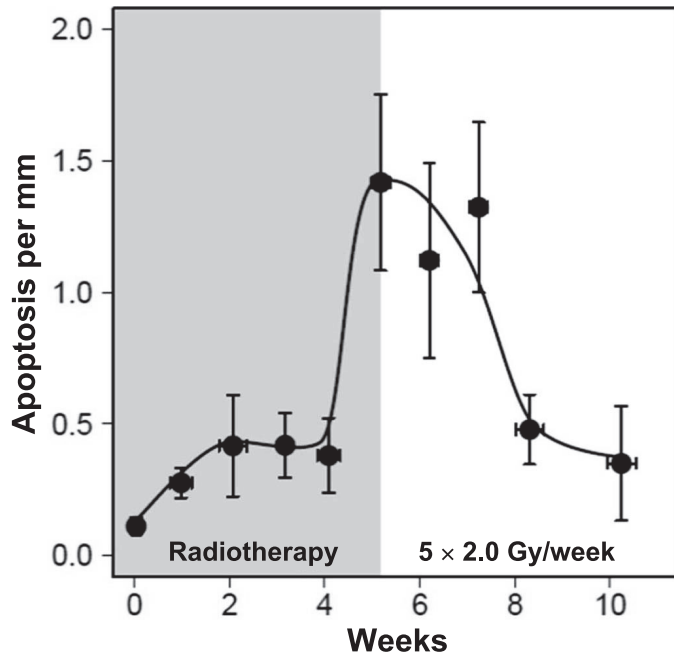
FIG. 10. Apoptotic cells in the basal and suprabasal layers, identified by homogeneous staining with γ-H2AX, induced by daily 2 Gy fractions for 5 weeks. Vertical error bars indicate the standard error of the mean for the number of apoptotic cells per mm. Horizontal error bars indicate the standard deviation of the biopsy acquisition time.

keratinocytes that lasted for a couple of weeks, followed by a greater cell loss rate in the second half of the treatment course (Fig. 2 and 3A); this pattern was confirmed by hypofractionation, using 4×2.4 Gy/week and 2×4 Gy/week over 5 weeks (Figs. 3C and D).

Evidence of a non-exponential cell loss rate of basal keratinocytes was previously established for daily fractions of 1.10 Gy over 7 weeks; a slightly downward curve was recorded, but in this case, it was less pronounced than after daily 2.0 Gy fractions, as shown in Fig. 2. On the other hand, for daily fractions of 0.07, 0.18 and 0.44 Gy, the rate of keratinocyte loss was strictly exponential, and the slope increased with increasing fraction size (*8*). There is some evidence suggesting changes in the growth fraction during the radiotherapy course, which might explain the dose per fraction-dependent behavior of the depletion rate for basal keratinocytes in skin (*27*).

Changes in Growth Fraction and Proliferative Capacity

Preliminary findings regarding changes in the growth fraction of basal keratinocytes during radiotherapy with daily 2 Gy fractions as assessed by Ki67 and cyclinA staining have been described elsewhere for group 1 patients (*28*). A complete assessment of basal keratinocyte proliferation using staining of Ki67, cyclinA and cyclinB in biopsies from all 31 patients in this study has now been performed.[3] The Ki67 protein is present only in cycling

[3] Unpublished results.

cells, i.e., it is absent in the G_0 phase. Its expression increases with progression through the cell cycle. The Ki-67 count, including early G_1 cells with the weakest staining, thus provides an estimate of the growth fraction (*28, 29*). These analyses suggest that after initial, almost complete suppression of the number of cycling cells, which lasts a couple of weeks, there is accelerated recruitment of cells into the cell cycle and accumulation of cells in G_1 and G_2 during the final 2 weeks of radiotherapy. The growth fraction therefore is substantially depressed compared to baseline for the first couple of weeks, but then increases successively over the latter part of treatment. Before radiotherapy, the growth fraction was approximately 15%, only a few percentages at 2 weeks, and approximately 35% towards the end of the week 5. A very similar pattern was observed for the 5-week hypofractionation schedules, and also for 2×2.0 Gy per day, although that treatment was completed at 2.5 weeks for this schedule.[3]

Of note, however, the current study emphasizes that the emerging larger growth fraction during the latter part of the treatment did not suggest a corresponding increase in mitosis; rather, the absolute number of mitoses was significantly suppressed during the entire treatment period (Fig. 6). Proliferation expressed as mitotic index was 0.46% before radiotherapy, 0.10% at 2 weeks and 0.37% at the end of treatment. When the changes in growth fraction are compared with those in the mitotic index, it is evident that the accelerated recruitment of cells into the cell cycle after a couple of weeks of radiotherapy is not synonymous with accelerated repopulation. An unexpected finding was the substantial redistribution of cells from quiescence (G_0) into the cell cycle (*28*)[3], but these cells have a limited capacity to divide as long as radiation treatment is underway (Fig. 6). The most reasonable interpretation of this phenomenon is that cycling cells become, to a great extent, permanently arrested at the G_1 and G_2 checkpoints. Subsequently, these cells exit the cell cycle and migrate upwards from the basal to the superficial layers, maintaining their differentiation capability (*13, 14*). This phenomenon was reflected in the preserved and even thickening of the cornified cell layer observed during ongoing treatment (Fig. 5B). Furthermore, the substantial increase in apoptosis observed at the end of radiotherapy (Fig. 10), without a corresponding increase in mitosis (Fig. 6), probably reflects an increasing propensity of primary apoptosis because of a high accumulation of DSBs in subpopulations of arrested cells (Figs. 7 and 8).

During the first treatment weeks, the proliferation in the basal cell layer was strongly suppressed, independent of the fractionation schedule. Therefore, when treatment with 2×2.0 Gy per day was given to 50 Gy in 2.5 weeks, the vast majority of basal keratinocytes rested in the G_0 phase during the entire treatment course. The rate of cell depletion during this period was as low as for daily fractions of 2.0 Gy in the first half of radiotherapy (Figs. 3A and B). These results suggest negligible elimination of cells from the G_0 phase, and thus a low radioresponsiveness of quiescent cells,

independent of dose intensity, which also was the case for hypofractionation (Fig. 3C and D).

In the subsequent weeks, in parallel to stimulated recruitment of cells into the cell cycle, the keratinocyte depletion rate increased, but was less pronounced for 2.0 Gy fractions given twice daily compared to once daily (Fig. 3A and B). The outcome after completion of the twice-daily regimen suggests that cells exit G_0 and enter G_1 in the presence of unrepaired DNA damage; indeed, these cells were eliminated from the cell cycle and the basal layer at a rate that did exceed the cell production rate through successful mitoses. When daily 2.0 Gy radiation fractions were delivered in this period of forced recruitment of G_0 cells into the cell cycle, a substantial increase in the depletion rate occurred. The subpopulation of cycling keratinocytes contributed to a higher radioresponsiveness for several reasons: entry into the cell cycle of cells with residual DSBs, increased sensitivity to DSBs in cycling compared to non-cycling cells (discussed below), and the probability of accumulation of DSBs at cell cycle-specific checkpoints. The ability of these cells to proceed through the cell cycle depends on the efficacy of the checkpoints in G_1/S and G_2/M transitions during the period of enforced proliferation. However, the simultaneous suppression of mitosis (Fig. 6) suggests that these checkpoints are also quite effective under this condition, and limit the proliferative capacity as long as the radiation treatment is underway.

In addition, by comparing the cell loss rate for 2.0 Gy given twice daily with once-daily administration, evidence of compensatory proliferation of basal keratinocytes was not apparent during the latter half of the 5-week treatment. The nadir for 50 Gy in 2.5 weeks was significantly less than for 50 Gy in 5 weeks (Fig. 3A and B), which is also an indication of increasing radioresponsiveness rather than sparing by repopulation during treatment with the latter schedule. Surprisingly, the nadir appeared at 6 weeks from treatment start in both cases, supporting the notion that surviving cells in quiescence (G_0) at the end of treatment account for the accelerated repopulation that is not observed until a period of time after radiotherapy cessation (Fig. 6).

The current study brings attention to significant changes in radioresponsiveness of basal skin keratinocytes during 5-week radiation treatment with daily 2 Gy fractions; the first half of the treatment reflects low responsiveness of G_0 cells, and the latter part reflects high responsiveness of cells induced into active proliferation. Compensatory repopulation could not be confirmed. This picture agrees with and supportive of the outcome in a clinical study showing a significantly stronger acute skin reaction after 50 Gy in 5 weeks compared to 50 Gy in 2.5 weeks (2 Gy twice daily, 8-h interval) using scoring of desquamation as the end point (30). Altogether, this scenario speaks against the use of a separate time factor, expressed in Gy/day, in the interpretation of the biological effect of a particular fractionation schedule concerning acute reactions in epithelium.

The dilemma in interpreting the response of basal keratinocytes correctly is related to the lack of knowledge about the features of these cells concerning proliferative ability. Proliferation of epidermal keratinocytes occurs for the most part in the basal layer. Basal keratinocytes display heterogeneity in proliferation rate and capacity. A wealth of data suggests that basal keratinocytes comprise rare stem cells (SCs), expanding populations of transient amplifying (TA)/committed progenitor (CP) cells and early differentiating cells. These three distinct subsets were characterized by the cell surface receptors α6bri CD71dim, α6bri CD71bri and α6dim, respectively, and were shown to be molecularly distinct. Because of the lack of a unique marker for SCs, there is still no way to clearly identify them (31–33).

Stem cells are supposed to have unlimited proliferative ability, while the progenitors gradually lose this capacity in differentiation. This association was supported by an elegant study on the interfollicular epidermis of neonatal human foreskin (34). Under steady-state conditions, SCs are quiescent and divide only occasionally through asymmetric duplication into a SC and a progenitor cell. Recently published studies revealed that wound repair involves activating SCs, resulting in an increase in the proliferation rate while keeping the asymmetric mode of division that gives rise to progenitors. The increasing number of progenitor cells was not associated with increase in their self-renewal capacities but rather with a massive depletion through differentiation. These authors concluded that only SCs contribute substantially to repair and long-term regeneration of tissue, whereas committed progenitor cells make a limited contribution (35, 36).

The role of epidermal SCs for acute skin reactions was reviewed in detail recently (37). In the clinic, rapidly growing macroscopic colonies have been observed only in irradiated areas that showed moist desquamation, i.e., almost total depletion of epidermal cells (38). This situation is similar to that of wound healing, i.e., SCs will be recruited into the cell cycle when extensive tissue regeneration is required. The CD71 receptor as well as the epidermal growth factor receptor correlates with mitotic activity of basal keratinocytes (39). The lower expression of both in SCs compared to TA/CP cells indicates that mitogenic stimulation upon radiation damage initially recruits TA/CP cells into the cell cycle. Proliferative activation of SCs is expected to occur gradually with increasing skin reaction but will not be apparent until there is severe denudation of basal cells. In this study using 50 Gy radiation, the number of basal keratinocytes was reduced to only approximately 50% at the end of treatment. Therefore, at this time point the majority of remaining cells still comprised TA/CP cells and early differentiating cells, and SCs would not be fully stimulated to cell cycle entry. We suggest that this is a reasonable explanation for why significant repopulation of SCs did not occur during the radiotherapy course (Fig. 6).

Concerning the radiosensitivity of basal keratinocytes, *ex vivo* irradiation has revealed that SCs (α6bri CD71dim) are more radioresistant than TA/CP cells (α6bri CD71bri), sorted from human foreskin. This result could partly be explained by different radiation-induced gene expressions, indicating a higher DSB repair capacity and a reduced apoptotic response for SCs compared to TA/CP cells (*40*). Altogether, the response of basal keratinocytes to moderate doses, such as 50 Gy in 5 weeks used in this study, resulting in dry desquamation, is expected to be determined by the more radiosensitive TA/CP cells, which preferentially are depleted by premature differentiation provoked by arrest at cell cycle-specific DNA damage checkpoints.

A limitation of the current study is the rather low-dose level of 50 Gy. With increasing doses, the SCs will have an increasing effect on response. However, the fate of cycling SCs is virtually unknown both concerning the radiosensitivity within the cell cycle and their sensitivity to cell cycle-specific checkpoints. Therefore, the current findings should not be extrapolated beyond moderate doses or to other types of epithelium.

Growth Arrest and DNA Damage

The results for the nuclear expression of the p21 protein, which reflects the growth arrest of germinal keratinocytes, also indicate a biphasic increase in the number of p21-positive cells (Fig. 5A), which increased faster during the second half of the treatment course. A previously published study involving daily fractions of 1.10 Gy (*27*) suggested that the p21 response is related to the proportion of cells within the cell cycle, i.e., the growth fraction.

The p21 protein is the principal mediator of the G_1 checkpoint in response to DNA damage. p21 causes G_1 arrest by inhibiting the activity of cyclin/CDK complexes required for the G_1/S-phase transition and by directly blocking DNA synthesis in the S phase through interactions with proliferating cell nuclear antigen. The p21 protein also plays a crucial role in the G_2 checkpoint. Specifically, p21 is essential in maintaining G_2 arrest in response to DNA damage via various mechanisms that prevent G_2-arrested cells from entering mitosis (*11, 12, 41*).

The increase in nuclear p21 protein levels is mediated by transcriptional activation of p53. DSBs activate the serine-threonine kinase ATM, which in turn phosphorylates p53 (directly or through CHK2) and MDM2, ensuring that both p53 protein expression and transcriptional activity of p53 will increase (*42–44*). The p53 response is approximately linearly correlated with the number of DSBs (*45*). Therefore, p21 protein levels are expected to be proportional to the number of DSBs. We found that both the number of p21-positive cells (Fig. 5 A) and p21-staining intensity increased during the treatment course with daily 2 Gy fractions (data not shown), as was previously proven for 1.1 Gy daily fractions (*8*), and well appeared in accordance with the increase in 53BP1 foci during the final 2 weeks of

radiotherapy (Fig. 7). As well, the biphasic increase in the number of p21-positive basal keratinocytes over the 5-week radiotherapy course should reflect changes in the growth fraction that increased substantially during the second half of the treatment (Fig. 5A) (*27*).

Recently published studies have revealed that the level of p21 induced by DNA damage determines the propensity to a permanent exit of G_2 cells. In addition, the level of p21 in cells that succeed to pass mitosis determines whether or not the cell will continue the cell cycle or enter into a quiescent state (*46–48*). A higher amount of p21 increases the risk of permanent G_2 exit and also the probability of entering quiescence after exit from mitosis. Thus, high levels of p21 may counteract efficient repopulation. However, this scenario will be offset by mitogen signaling triggered by successive depletion of germinal keratinocytes. The fate of the daughter cells depends on: 1. the degree of mitogen ERK-signaling and the induced amount of cyclin D1 mRNA; and 2. the degree of DNA damage-induced p53 activation, manifested in the mother cell as p21 expression. Whether the daughter cells enter the cell cycle or quiescence is critically balanced by the ratio between cyclin D1 and p21; the higher the ratio the higher probability of entering the cell cycle. Highly important in this context is that mitogen signaling also activates Myc, which in turn degrades p21 (*49, 50*), facilitating repopulation by increasing the cyclin D1 to p21 ratio. Interestingly, it is well known that suppression of p21 is required before cell cycle entry (*51*).

Furthermore, as soon as the radiation treatment was completed and the genotoxic exposure interrupted, p21 declined rapidly, indicating that the cyclinD1 to p21 ratio increased unimpededly, which explains the extensive cell division activity triggered after treatment (Fig. 6).

Altogether, based on the above, we assume that the p21-negative basal keratinocytes at the end of treatment belong to the G_0 compartment but are prepared to enter into the cell cycle because of mitogen pressure. Some of these cells might be the surviving cells that repopulate the basal keratinocyte cell layer, reflected in the peak of mitotic cells delayed until 2 weeks after completion of radiotherapy (Fig. 6).

Concerning the number of DSB foci, changes in cell cycle distribution probably also explain the striking variations in DSB foci per cell in the basal layer during radiotherapy (Fig. 7). In the manual analysis, a substantial reduction in 53BP1 foci per cell was found for dose fractions given at 1 and 2 weeks of radiotherapy compared to the very first dose fraction. Thus, the low response of keratinocyte loss in G_0 phase during the first treatment weeks was associated with diminished DSB sensitivity. In contrast, for dose fractions delivered towards the end of treatment, the number of 53BP1 foci per cell increased significantly compared to the very first fraction of 2.0 Gy. Thus, the increasing response of keratinocyte loss that occurred in parallel with increasing growth fraction was associated with greater DSB sensitivity.

The variability in DSB foci for keratinocytes during treatment is also dependent on the effect of chromatin compaction. The number of γ-H2AX foci induced per unit dose is several times higher in decondensed euchromatin in cycling cells compared to compact heterochromatin in G_0 cells (52, 53). Cell entry into quiescence results in more tightly packed chromatin that is reversibly unpacked upon stimulation of the cell to reenter the cell cycle (54). Therefore, cells in the G_0 phase are expected to be more radioresistant to DSB induction than if they are cycling.

Of interest, the current study showed that the number of 53BP1 foci per cell for keratinocytes in the basal layer was significantly higher at 30 min after the very first fraction than after fractions delivered during the first and second weeks of radiotherapy. This pattern can probably be ascribed to changes in chromatin structure at the different time points. At the start of radiotherapy, the number of cycling cells is significantly higher than at the first and second weeks, when almost all cells are in G_0 (28). Furthermore, at the start of radiotherapy, cycling basal keratinocytes are mainly in the G_1 phase; too few cells are in the G_2 phase to affect the induction of DSBs (discussed below). Therefore, the 53BP1 foci assessment during the first two weeks of radiotherapy revealed that cycling cells already in G_1 are more sensitive to DSBs than quiescent cells.

In addition to the effect of chromatin structure that influences the DSB induction differently for cycling and non-cycling cells, two more explanations were identified for the increase in DSB foci density during the latter half of the radiotherapy treatment (Fig. 7). First, the assessment of 53BP1 foci in the group 1 patients indicated persistent DSB foci after 24 h, just before the next dose fraction of radiotherapy; these foci accumulated over time when daily dose fractions are given. Second, recruitment of cells into the cell cycle after a couple of weeks of treatment causes an increasing proportion of cells to accumulate in G_2 arrest.[3] In G_2 cells, the DNA and chromatin content is doubled compared to G_0 and G_1 cells. Consequently, the number of DSBs induced per unit dose is twofold in G_2. Therefore, changes in cell cycle distribution and the accumulation of cells in G_2 arrest affect the density of DSB foci (23).

To elucidate different methods for assessing DSBs in epithelium, immunofluorescence and digital image analysis of DSB foci per nuclear area, as an average of all nucleated epidermal cells, was performed by staining with 53BP1 and γ-H2AX (Fig. 8). In contrast to the manual counting, the effect of a reduced growth fraction in the basal layer between the first dose fraction and fractions delivered at 1 and 2 weeks was not observed with image analysis. This absence may be explained by the fact that the proliferating basal cells comprise a minor portion of the cells in epidermis at this point in time. However, during the second half of treatment, the image analysis revealed an increase in the average foci density in epidermal cell layers, confirming the finding from the manual counting of 53BP1 foci in basal

cells. In addition to a relative increase of G_2 cells in the basal layer during this period, permanently arrested G_2 cells are assumed to exit the cell cycle and migrate upwards into the differentiated cell layers, keeping their double DNA content. Therefore, the proportion of nucleated epidermal cells with double DNA content increased during the latter part of the radiotherapy course, which might be reflected in the increasing DNA foci density in this period (Fig. 8).

In our experience, the immunofluorescence staining of 53BP1 produces a far stronger signal compared to the signal from γ-H2AX staining. Nonspecific background staining is very weak for γ-H2AX, and in terms of intensity, the dynamic range for different 53BP1 foci is greater than for γ-H2AX foci. Because 53BP1 is always present in the cell nucleus and the antibody is very sensitive, some foci-like structures may be observed, resulting in what would be perceived as higher foci density in nonirradiated controls. In theory, γ-H2AX staining should be more specific than 53BP1 staining. The antibody against γ-H2AX is a phospho-specific antibody, so the background signal should be low. However, the formalin fixation of the biopsies had a negative effect on the signal (Fig. 9); consequently, the signal-to-noise ratio was still lower than that of 53BP1.

There is support for the current findings in the literature. Evidence of accumulation of unrepaired DSBs as assessed by γ-H2AX staining has been established for various acute- and late-responding tissues in mice receiving 3 to 5 daily fractions of 2 Gy (55). Most important, using the same clinical assay as ours, Somaiah et al. (56) showed an accumulation of basal keratinocytes in S and G_2 phases after 2 Gy daily fractions given over 5 weeks. Similar to our findings, the majority of cells expressed p21 at the end of treatment, and there was an associated increase in RAD51 foci. RAD51 foci are an indication of ongoing homologous recombination (HR) of DSBs, induced in S and G_2, while 53BP1 foci represent existence of non-homologous end-joining of DSBs. HR is expected to be effective in S and G_2, while the capability of non-homologous end-joining is reduced due to BRCA1 suppression of 53BP1 (57). However, in the current study, a larger amount of 53BP1foci was recorded during the latter part of treatment enriched with G_2 cells (Figs. 7 and 8) and manifested the more pronounced radiosensitivity of basal keratinocytes. Therefore, clinically the protective effect of HR during the latter half of the 5-week treatment appears to be limited. Also, there remains some uncertainty as to whether the diminishing fractionation sensitivity, established a long time ago for acute skin reaction in radiotherapy courses lasting longer than 4 weeks (58), is a result of HR, as suggested by Somaiah et al. (56). Alternatively, observations from this study suggest that decreasing fractionation sensitivity might be explained by accumulation of unrepaired DSBs between daily fractions in cells arrested at both the G_1/S and G_2/M transitions. This scenario will probably lead to permanent checkpoint arrests and premitotic elimination of cycling

cells. Only a few cells appear to recover sufficiently to enter mitosis during the course of radiation treatment (Fig. 6).

The lack of obvious repopulation of basal keratinocytes throughout the entire treatment period is in line with the fact that no significant time factor for acute skin erythema and desquamation could be established for overall treatment times up to 6 weeks, when different clinical fractionation schedules were investigated (*58*).

Cell Death

Cell death was assessed by identifying cells with intense and homogeneous γ-H2AX fluorescent immunostaining. This marker co-localizes with cleaved PARP-1 in the epidermis and shows a distinct staining pattern in cells undergoing apoptosis (*17*). The TUNEL assay is commonly used to assess apoptosis in skin. However, in our hands this staining was not sufficient for accurate quantification of apoptotic cells.

With the use of the γ-H2AX assay, apoptotic events were infrequent but higher than in unexposed skin over the first 4 weeks of radiotherapy with daily fractions of 2 Gy. However, in a numerical comparison of Figs. 6 and 10, the increase in apoptotic cells matched the decrease in mitotic cells in this period and probably reflects cell killing of mitotic cells, as DSBs induced in these cells are unrepairable (*59*).

In contrast and unexpectedly, there was a pronounced increase in apoptotic cells per mm during the last few fractions. Of note, there was no corresponding increase in the number of mitotic cells per mm at this time. Therefore, the peak in apoptosis is probably not secondary to mitotic failure. Rather, we suggest that the accumulation of DSBs in subpopulations of basal keratinocytes is high enough to trigger apoptosis before entry into mitosis. In contrast, the increased number of apoptotic events that occur a couple of weeks after completion of radiotherapy is associated with a high mitotic rate. It is likely that these apoptotic cells are generated from mitotic cell death of SCs as a result of unrepaired DSBs inflicted during the treatment course.

Dose Response of Melanocyte Number

Previously we showed that melanocytes were radioresistant regarding depletion during 7 weeks of radiotherapy with daily dose fractions in the range 0.05–1.10 Gy. We could also state that neither apoptosis nor proliferation did occur, and presented clear evidence that cells of the melanocyte lineage responded with differentiation (*18*). In the current study, the number of melanocytes also remained undisturbed by adjuvant radiotherapy and the use of daily 2 Gy fractions for 5 weeks, and for hypo- and accelerated fractionation as well. In agreement with the findings for daily fractions up to 1.10 Gy, the melanocytes rarely expressed nuclear p21 protein after dose fractions of 2–4 Gy. The molecular pathways that suppress the p53-p21 pathway in melanocytes are only partly understood and

have been discussed previously elsewhere (*18*). Further investigations of the molecular response of the melanocytes are underway.

Concluding Remarks

This study did not confirm accelerated repopulation during a five-week treatment course in the germinal keratinocyte cell layer of epidermis. Rather, a significant proliferative suppression occurred throughout the treatment. The outcome highlights the efficacy of cell cycle check-points to induce permanent cell growth arrest in normal squamous epithelium while exposed to moderate radiation doses. p21 has an outstanding role in counteracting repopulation upon genotoxic exposure, not only by exerting cell cycle stop in the G_1/S and G_2/M transitions, but also by governing the decision between quiescence and cell cycle entry of daughter cells passing mitosis.

Recent preclinical knowledge of epidermal tissue regeneration and cell cycle progression during genotoxic and mitogen stress allows credible explanation of the current finding. In particular, the fact that the p53/p21 pathway was recently proven to regulate cell proliferation and repopulation during exposure to genotoxic stress in normal epithelium, will have therapeutic implications for malignancies that lack p53 function, which accordingly will have the potential to permit uncontrolled repopulation.

The number of interfollicular melanocytes is untouched by adjuvant radiotherapy to dose levels approximately equivalent to daily 2 Gy fractions for 5 weeks.

REFERENCES

1. Withers HR. Recovery and repopulation in vivo by mouse skin epithelial cells during fractionated irradiation. Radiat Res 1967; 32:227–39.

2. Fowler JF, Morgan RL, Silvester JA, Bewley DK, Turner BA. Experiments with fractionated x-ray treatment of the skin of pigs. Br J Radiol 1963; 36:188–96.

3. Denekamp J. Changes in the rate of repopulation during multifraction irradiation of mouse skin. Br J Radiol 1973; 46:381–7.

4. Morris GM, Hopewell JW. Changes in the cell kinetics of pig epidermis after repeated daily doses of X rays. Br J Radiol Suppl 1986; 19:34–8.

5. Archambeau JO, Hauser D, Shymko RM. Swine basal cell proliferation during a course of daily irradiation, five days a week for six weeks (6000 rad). Int J Radiat Oncol Biol Phys 1988; 15:1383–8.

6. Thames HD, Hendry JH. Fractionation in radiotherapy: London-New York-Philadelphia: Taylor & Francis; 1987.

7. Dorr W. Time factors in normal-tissue responses to irradiation. In: Joiner M, van der Kogel A, editors. Basic clinical radiobiology. 4th ed. London-New York-Philadelphia: Taylor & Francis/Hodder Arnold; 2009.

8. Turesson I, Nyman J, Qvarnstrom F, Simonsson M, Book M, Hermansson I, et al. A low-dose hypersensitive keratinocyte loss in response to fractionated radiotherapy is associated with growth arrest and apoptosis. Radiother Oncol 2010; 94:90–101.

9. Qvarnstrom F, Simonsson M, Nyman J, Hermansson I, Book M, Johansson KA, et al. Double strand break induction and kinetics indicate preserved hypersensitivity in keratinocytes to subtherapeutic doses for 7 weeks of radiotherapy. Radiother Oncol 2017; 122:163–9.

10. Harper JW, Elledge SJ, Keyomarsi K, Dynlacht B, Tsai LH, Zhang P, et al. Inhibition of cyclin-dependent kinases by p21. Mol Biol Cell 1995; 6:387–400.

11. Cazzalini O, Scovassi AI, Savio M, Stivala LA, Prosperi E. Multiple roles of the cell cycle inhibitor p21(CDKN1A) in the DNA damage response. Mutat Res 2010; 704:12–20.

12. Shaltiel IA, Krenning L, Bruinsma W, Medema RH. The same, only different - DNA damage checkpoints and their reversal throughout the cell cycle. J Cell Sci 2015; 128:607–20.

13. von Wangenheim KH, Peterson HP, Schwenke K. Review: a major component of radiation action: interference with intracellular control of differentiation. Int J Radiat Biol 1995; 68:369–88.

14. Weinberg WC, Denning MF. P21Waf1 control of epithelial cell cycle and cell fate. Crit Rev Oral Biol Med 2002; 13:453–64.

15. Brown JM, Wouters BG. Apoptosis, p53, and tumor cell sensitivity to anticancer agents. Cancer Res 1999; 59:1391–9.

16. Steel GG. The case against apoptosis. Acta Oncol 2001; 40:968–75.

17. Simonsson M, Qvarnstrom F, Nyman J, Johansson KA, Garmo H, Turesson I. Low-dose hypersensitive gammaH2AX response and infrequent apoptosis in epidermis from radiotherapy patients. Radiother Oncol 2008; 88:388–97.

18. Fessé P, Qvarnstrom F, Nyman J, Hermansson I, Ahlgren J, Turesson I. UV-radiation response proteins reveal undifferentiated cutaneous interfollicular melanocytes with hyperradiosensitivity to differentiation at 0.05 Gy radiotherapy dose fractions. Radiat Res 2019; 191:93–106.

19. Nyman J, Turesson I. Basal cell density in human skin for various fractionation schedules in radiotherapy. Radiother Oncol 1994; 33:117–24.

20. Johnson JL, Najor NA, Green KJ. Desmosomes: regulators of cellular signaling and adhesion in epidermal health and disease. Cold Spring Harb Perspect Med 2014; 4:a015297.

21. Hirata A, Inada K, Tsukamoto T, Sakai H, Mizoshita T, Yanai T, et al. Characterization of a monoclonal antibody, HTA28, recognizing a histone H3 phosphorylation site as a useful marker of M-phase cells. J Histochem Cytochem 2004; 52:1503–9.

22. Rogakou EP, Pilch DR, Orr AH, Ivanova VS, Bonner WM. DNA double-stranded breaks induce histone H2AX phosphorylation on serine 139. J Biol Chem 1998; 273:5858–68.

23. Lobrich M, Shibata A, Beucher A, Fisher A, Ensminger M, Goodarzi AA, et al. gammaH2AX foci analysis for monitoring DNA double-strand break repair: strengths, limitations and optimization. Cell Cycle 2010; 9:662–9.

24. Schultz LB, Chehab NH, Malikzay A, Halazonetis TD. p53 binding protein 1 (53BP1) is an early participant in the cellular response to DNA double-strand breaks. J Cell Biol 2000; 151:1381–90.

25. Panier S, Boulton SJ. Double-strand break repair: 53BP1 comes into focus. Nat Rev Mol Cell Biol 2014; 15:7–18.

26. Qvarnstrom OF, Simonsson M, Johansson KA, Nyman J, Turesson I. DNA double strand break quantification in skin biopsies. Radiother Oncol 2004; 72:311–7.

27. Turesson I, Bernefors R, Book M, Flogegard M, Hermansson I, Johansson KA, et al. Normal tissue response to low doses of radiotherapy assessed by molecular markers–a study of skin in patients treated for prostate cancer. Acta Oncol 2001; 40:941–51.

28. Hopewell JW, Nyman J, Turesson I. Time factor for acute tissue reactions following fractionated irradiation: a balance between repopulation and enhanced radiosensitivity. Int J Radiat Biol 2003; 79:513–24.

29. Scholzen T, Gerdes J. The Ki-67 protein: from the known and the unknown. J Cell Physiol 2000; 182:311–22.

30. Nyman J, Turesson I. Does the interval between fractions matter in the range of 4–8 h in radiotherapy? A study of acute and late human skin reactions. Radiother Oncol 1995; 34:171–8.

31. Potten CS. The epidermal proliferative unit: the possible role of the central basal cell. Cell Tissue Kinet 1974; 7:77–88.

32. Webb A, Li A, Kaur P. Location and phenotype of human adult keratinocyte stem cells of the skin. Differentiation 2004; 72:387–95.

33. Fuchs E. Epithelial Skin Biology: Three Decades of Developmental Biology, a Hundred Questions Answered and a Thousand New Ones to Address. Curr Top Dev Biol 2016; 116:357–74.

34. Schluter H, Paquet-Fifield S, Gangatirkar P, Li J, Kaur P. Functional characterization of quiescent keratinocyte stem cells and their progeny reveals a hierarchical organization in human skin epidermis. Stem Cells 2011; 29:1256–68.

35. Mascre G, Dekoninck S, Drogat B, Youssef KK, Brohee S, Sotiropoulou PA, et al. Distinct contribution of stem and progenitor cells to epidermal maintenance. Nature 2012; 489:257–62.

36. Aragona M, Dekoninck S, Rulands S, Lenglez S, Mascre G, Simons BD, et al. Defining stem cell dynamics and migration during wound healing in mouse skin epidermis. Nat Commun 2017; 8:14684.

37. Martin MT, Vulin A, Hendry JH. Human epidermal stem cells: Role in adverse skin reactions and carcinogenesis from radiation. Mutat Res 2016; 770:349–68.

38. Arcangeli G, Mauro F, Nervi C, Withers HR. Dose-survival relationship for epithelial cells of human skin after multifraction irradiation: evaluation by a quantitative method in vivo. Int J Radiat Oncol Biol Phys 1980; 6:841–4.

39. Fortunel NO, Martin MT. Cellular organization of the human epidermal basal layer: clues sustaining a hierarchical model. Int J Radiat Biol 2012; 88:677–81.

40. Rachidi W, Harfourche G, Lemaitre G, Amiot F, Vaigot P, Martin MT. Sensing radiosensitivity of human epidermal stem cells. Radiother Oncol 2007; 83:267–76.

41. Bunz F, Dutriaux A, Lengauer C, Waldman T, Zhou S, Brown JP, et al. Requirement for p53 and p21 to sustain G2 arrest after DNA damage. Science 1998; 282:1497–501.

42. el-Deiry WS, Tokino T, Velculescu VE, Levy DB, Parsons R, Trent JM, et al. WAF1, a potential mediator of p53 tumor suppression. Cell 1993; 75:817–25.

43. Bakkenist CJ, Kastan MB. DNA damage activates ATM through intermolecular autophosphorylation and dimer dissociation. Nature 2003; 421:499–506.

44. Pereg Y, Shkedy D, de Graaf P, Meulmeester E, Edelson-Averbukh M, Salek M, et al. Phosphorylation of Hdmx mediates its Hdm2- and ATM-dependent degradation in response to DNA damage. Proc Natl Acad Sci U S A 2005; 102:5056–61.

45. Loewer A, Karanam K, Mock C, Lahav G. The p53 response in single cells is linearly correlated to the number of DNA breaks without a distinct threshold. BMC Biol 2013; 11:114.

46. Spencer SL, Cappell SD, Tsai FC, Overton KW, Wang CL, Meyer T. The proliferation-quiescence decision is controlled by a bifurcation in CDK2 activity at mitotic exit. Cell 2013; 155:369–83.

47. Arora M, Moser J, Phadke H, Basha AA, Spencer SL. Endogenous replication stress in mother cells leads to quiescence of daughter cells. Cell Rep 2017; 19:1351–64.

48. Yang HW, Chung M, Kudo T, Meyer T. Competing memories of mitogen and p53 signalling control cell-cycle entry. Nature 2017; 549:404–8.

49. Mitchell KO, el-Deiry WS. Overexpression of c-Myc inhibits p21WAF1/CIP1 expression and induces S-phase entry in 12-O-tetradecanoylphorbol-13-acetate (TPA)-sensitive human cancer cells. Cell Growth Differ 1999; 10:223–30.

50. Seoane J, Le HV, Massague J. Myc suppression of the p21(Cip1) Cdk inhibitor influences the outcome of the p53 response to DNA damage. Nature 2002; 419:729–34.

51. Nakanishi M, Adami GR, Robetorye RS, Noda A, Venable SF, Dimitrov D, et al. Exit from G0 and entry into the cell cycle of cells expressing p21Sdi1 antisense RNA. Proc Natl Acad Sci U S A 1995; 92:4352–6.

52. Falk M, Lukasova E, Kozubek S. Chromatin structure influences the sensitivity of DNA to gamma-radiation. Biochim Biophys Acta 2008; 1783:2398–414.

53. Takata H, Hanafusa T, Mori T, Shimura M, Iida Y, Ishikawa K, et al. Chromatin compaction protects genomic DNA from radiation damage. PLoS One 2013; 8:e75622.

54. Evertts AG, Manning AL, Wang X, Dyson NJ, Garcia BA, Coller HA. H4K20 methylation regulates quiescence and chromatin compaction. Mol Biol Cell 2013; 24:3025–37.

55. Rube CE, Fricke A, Wendorf J, Stutzel A, Kuhne M, Ong MF, et al. Accumulation of DNA double-strand breaks in normal tissues after fractionated irradiation. Int J Radiat Oncol Biol Phys 2010; 76:1206–13.

56. Somaiah N, Yarnold J, Daley F, Pearson A, Gothard L, Rothkamm K, et al. The relationship between homologous recombination repair and the sensitivity of human epidermis to the size of daily doses over a 5-week course of breast radiotherapy. Clin Cancer Res 2012; 18:5479–88.

57. Bakr A, Kocher S, Volquardsen J, Reimer R, Borgmann K, Dikomey E, et al. Functional crosstalk between DNA damage response proteins 53BP1 and BRCA1 regulates double strand break repair choice. Radiother Oncol 2016; 119:276–81.

58. Turesson I, Thames HD. Repair capacity and kinetics of human skin during fractionated radiotherapy: erythema, desquamation, and telangiectasia after 3 and 5 year's follow-up. Radiother Oncol 1989; 15:169–88.

59. Giunta S, Belotserkovskaya R, Jackson SP. DNA damage signaling in response to double-strand breaks during mitosis. J Cell Biol 2010; 190:197–207.